

# Test-beam studies of diamond sensors for SLHC

<sup>a</sup>Lorenzo Uplegger\*, <sup>b</sup>Jennifer Ngadiuba, <sup>c</sup>Enver Alagoz, <sup>a</sup>Jeff Andresen, <sup>c</sup>Kirk Arndt, <sup>c</sup>Gino Bolla, <sup>c</sup>Daniela Bortoletto, <sup>d</sup>Jean Marie Brom, <sup>e</sup>Richard Brosius, <sup>c</sup>Mayur Bubna, <sup>a</sup>John Chramowicz, <sup>f</sup>John Cumalat, <sup>f</sup>Frank Jensen, <sup>c</sup>Alex Krzywda, <sup>e</sup>Ashish Kumar, <sup>a</sup>Simon Kwan, <sup>a</sup>CM Lei, <sup>b</sup>Dario Menasce, <sup>b</sup>Luigi Moroni, <sup>g</sup>Margherita Obertino, <sup>h</sup>Ilya Osipenkov, <sup>i</sup>Lalith Perera, <sup>a</sup>Alan Prosser, <sup>a</sup>Ryan Rivera, <sup>g</sup>Ada Solano, <sup>a</sup>Ping Tan, <sup>b</sup>Stefano Terzo, <sup>a</sup>Nhan Tran, <sup>f</sup>Stephen Robert Wagner

*a. Fermi National Laboratory*

*b. Istituto Nazionale di Fisica Nucleare, Sezione di Milano Bicocca*

*c. Purdue University*

*d. Institut Pluridisciplinaire Hubert Curien Strasbourg*

*e. University of Buffalo*

*f. University of Colorado Boulder*

*g. Istituto Nazionale di Fisica Nucleare, Sezione di Torino*

*h. Texas A&M*

*i. Mississippi University*

## Abstract:

Diamond sensors are studied as an alternative to silicon sensors to withstand the high radiation doses that are expected in future upgrades of the pixel detectors for the SLHC. Diamond pixel sensors are intrinsically radiation hard and are considered as a possible solution for the innermost tracker layers close to the interaction point where current silicon sensors cannot cope with the harsh radiation environment. An effort to study possible candidates for the upgrades is undergoing using the Fermilab test-beam facility, FTBF, where diamonds and 3D silicon sensors have been studied. Using a CMS pixel-based telescope built and installed at the FTBF, we are studying charge collection efficiencies for un-irradiated and irradiated devices bump-bonded to the CMS PSI46 pixel readout chip. A description of the test-beam effort and preliminary results on diamond sensors will be presented.

*Key words: Tracking detectors, Diamond detectors, Solid state detectors, Test-beam*

## 1. Introduction\*

2  
3 The innermost tracking device of the CMS general purpose  
4 detector [1] at the Large Hadron Collider (LHC) at CERN,  
5 consists of three Barrel layers and four Forward disks whose  
6 basic building blocks are highly segmented silicon sensors  
7 (pixels) tightly coupled with their corresponding PSI46V2 [2]  
8 readout chips (ROCs). The high radiation doses that these  
9 devices will have to withstand after the future LHC upgrades  
10 is so high that the currently installed planar silicon sensors  
11 will be damaged too quickly to be a practical solution. In order  
12 to increase the radiation hardness of pixel detectors different  
13 strategies are being pursued and test-beam around the world  
14 are conducted to make sure that the performances of these  
15 sensors, after a heavy irradiation comparable to the doses that  
16 are envisioned at the SLHC, can still guarantee tracking  
17 capabilities to meet the physics goals. An effort to study  
18 possible candidates for the upgrades is undergoing at the  
19 Fermilab test-beam facility, FTBF, where diamonds and 3D  
20 silicon sensors are being studied. In this paper we'll focus our  
21 attention to the description of the test-beam architecture and to  
22 some preliminary results on diamond sensors.

23  
24  
25

## 262. Experimental setup

27  
28 The beam-tests were performed in 2012 at the FTBF with a  
29 120 GeV/c protons beam incident on an 8 planes pixel-  
30 detector telescope. This telescope consists of 8 modules  
31 leftover from the CMS Forward pixel detector production [2].  
32 They are based on the PSI46v2 Read Out Chip (ROC) [3],  
33 with 150  $\mu\text{m} \times 100 \mu\text{m}$  pixel size, arranged in two sections,  
34 with two Detectors Under Test (DUTs) placed between the  
35 two telescope stations. Enhanced resolution is derived from  
36 charge sharing by tilting the telescope planes at 25°. The  
37 telescope resolution on the DUTs is as small as 6  $\mu\text{m}$  both in  
38 X (150  $\mu\text{m}$ ) and Y (100  $\mu\text{m}$ ) coordinates.  
39 The Data Acquisition (DAQ) hardware is based on the  
40 CAPTAN system [4], developed at Fermilab, which uses a  
41 gigabit Ethernet link to transfer the data from the experimental  
42 area to the DAQ computer where data are stored. The  
43 software, also developed at Fermilab, runs on a Windows PC  
44 and is a suite of multithreaded applications written in C++. A  
45 Data Quality Monitor runs in parallel, while data are acquired  
46 to provide immediate feedback to spot any problem in real  
47 time.

## 493. Offline analysis

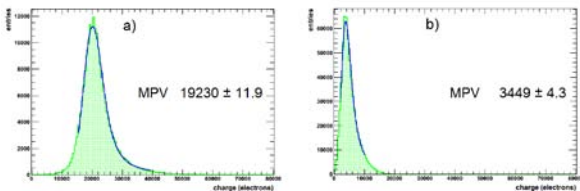
50  
51 In order to achieve the necessary resolution on the DUTs to  
52 allow for detailed studies on resolution and charge sharing,  
53 careful attention needs to be given to the alignment of the  
54 telescope and DUTs detectors in the beam. A dedicated  
55 software, called Monicelli, has been developed at the  
56 University of Milano Bicocca which achieves a track

\* This work was supported by Fermi National Accelerator Laboratory operated by Fermi Research Alliance, LLC under Contract No. DE-AC02-07CH11359 with the United States Department of Energy. L. Uplegger is with Fermi National Accelerator Laboratory, Batavia, IL 60510 USA (e-mail: uplegger@fnal.gov).

1 resolution on the DUTs as small as 6  $\mu\text{m}$ . Tracks are saved in  
 2 ROOT format to be later analyzed by another program, called  
 3 Chewie; the results of that analysis are discussed below.  
 4 We'll focus our attention on the preliminary results of 5  
 5 efficiency and charge collection for two diamond detectors,  
 6 both 500  $\mu\text{m}$  thick but with different crystal structure: mono  
 7 and poly crystalline.

#### 9 4. Charge collection

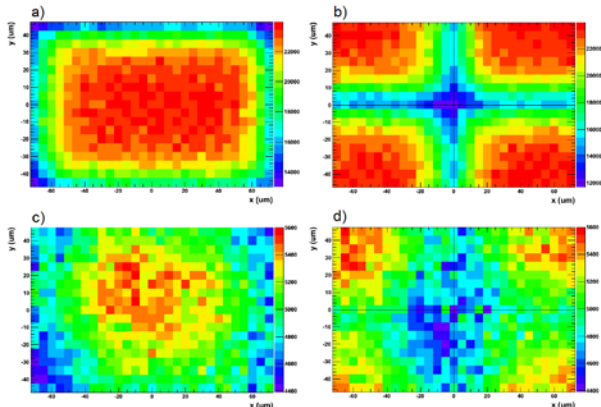
10  
 11 The charge collected in the two detectors varies greatly due  
 12 to the intrinsic nature of the two crystalline structures. The  
 13 mono-crystal has a charge collection distance (CCD) greater  
 14 than 500  $\mu\text{m}$  and the charge collected is thus around 20000  $e^-$   
 15 while the poly-crystal with its 172  $\mu\text{m}$  CCD only collects  
 16 about 3400  $e^-$  as the Landau charge profiles show in Figure 1.  
 17



18  
 19 **Figure 1:** a) Charge collected in the mono-crystal with most probable value  
 20 (MPV) around 20000  $e^-$  while b) is the charge collected in the poly-crystal with  
 21 MPV value around 3400  $e^-$ .

22  
 23 In Figure 2 instead we show the charge distribution in the  
 24 150  $\mu\text{m} \times 100 \mu\text{m}$  pixel cell for the two detectors. In these  
 25 sensors the charge drifts along the thickness of the detector  
 26 allowing the charge cloud to diffuse across pixels. Figure 2  
 27 shows that significant charge sharing is observed at 20  $\mu\text{m}$   
 28 where the charge collected by the pixel cell is lower than the  
 29 charge collected at the center. This effect is more evident in  
 30 Fig 3 where the charge collected at the corners of 4 pixel cells  
 31 is plotted.

32 Both mono and poly crystals show similar diffusion properties  
 33 with a cloud extending for 20-25  $\mu\text{m}$  with a slightly greater  
 34 diffusion cloud in the poly-crystal.  
 35

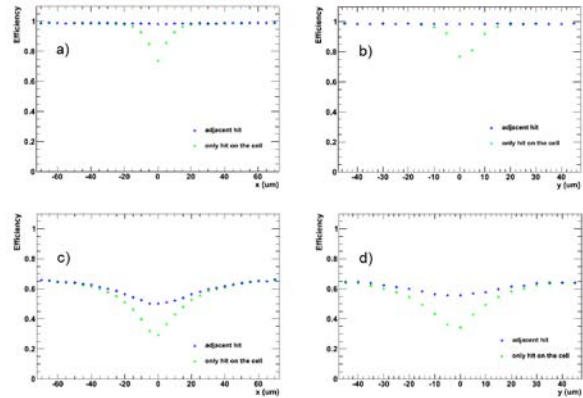


36  
 37 **Figure 2:** Plots a) and c) show the mean charge collected as a function of the  
 38 coordinates of the telescope predicted track impact point on a single pixel cell  
 39 for the mono and poly crystals respectively. Plots b) and d) show the mean  
 40 charge collected as a function of the coordinates of the track impact point  
 41 centered at the corner between four adjacent pixels for the mono and poly  
 42 crystals respectively.

#### 43 5. Efficiency

44  
 45 Efficiency measurements are strongly biased by the fact that  
 46 the amount of charge collected in the poly-crystal is just above  
 47 the minimum threshold of about 2400  $e^-$  that we could apply to

48 the ROC. Figure 3 shows the almost perfect efficiency for the  
 49 mono-crystal that reaches 99.8% and, on the other hand, the  
 50 low efficiency, due to threshold settings, of the poly-crystal  
 51 that is only around 65%. The two types of data points refer to  
 52 the sole efficiency of the pixel pointed by the track (green  
 53 points) and the combined efficiency of the two adjacent pixels  
 54 (blue points). While the combined efficiency, for the mono-  
 55 crystal, is constant and does not show any appreciable  
 56 degradation even in the region between pixels, for the poly-  
 57 crystal instead there is a further decrease in efficiency due to  
 58 the fact that the charge is split between two pixels thus  
 59 increasing the probability to be under threshold.  
 61



62  
 63 **Figure 3:** The green points show the detection efficiency of the sole pixel  
 64 pointed by the track as a function of the distance of the track impact point from  
 65 the boundary of the two adjacent pixels while the blue points show the combined  
 66 efficiency of the pixel pointed by the track and the adjacent one on the same  
 67 column, histograms a) for the mono-crystal, and c) for the poly-crystal, or on  
 68 the same row, histograms b) for the mono-crystal and d) for the poly-crystal.

#### 69 70 Conclusions

71  
 72 Preliminary results on two different, un-irradiated diamond  
 73 sensors tested extensively in a beam-test at Fermilab have  
 74 been shown in this paper. The purity of the mono-crystal  
 75 detector allows for a much higher charge collection distance  
 76 that results in the collection of a much higher quantity of  
 77 charge and thus showing very high detection efficiency  
 78 (99.8%). On the other hand, instead, the impurities in the poly-  
 79 crystalline structure of the other diamond detector limit the  
 80 amount of charge collected and thus results in poor  
 81 efficiencies (65%) since the ROC cannot be set at a threshold  
 82 far away from the Landau peak of this type of detector. Both  
 83 diamonds show similar charge diffusion properties though.

84  
 85 **Acknowledgments:** The authors would like to express  
 86 gratitude to the Fermilab test-beam facility personnel, and in  
 87 particular to Aria Soha, for their support during all test-beam  
 88 activities.

#### 89 90 Bibliography

- 91 [1] "The CMS Tracker Technical Design Report", CMS/LHC 98-6.  
 92 [2] "A Telescope Using CMS PSI46 Pixels and the CAPTAN for  
 93 Acquisition and Control over Gigabit Ethernet", R. A. Rivera,  
 94 M. Turqueti, L. Uplegger, 2009 IEEE Proc. Nuclear Science  
 95 Symposium.  
 96 [3] "Design and Performance of the CMS Pixel Detector Readout  
 97 Chip", H.C. Kästli et al, arXiv:physics/0511166.  
 98 [4] "CAPTAN: A hardware architecture for integrated data  
 99 acquisition, control, and analysis for detector development", M.  
 100 Turqueti et al, FERMILAB-PUB-08-527-CD